

Aligning Model Properties via Conformal Risk Control

William Overman^{*1}, Jacqueline Jil Vallon^{†2}, and Mohsen Bayati^{‡1}

¹Graduate School of Business, Stanford University

²Management Science and Engineering, Stanford University

Abstract

AI model alignment is crucial due to inadvertent biases in training data and the underspecified pipeline in modern machine learning, where numerous models with excellent test set metrics can be produced, yet they may not meet end-user requirements. Recent advances demonstrate that post-training model alignment via human feedback can address some of these challenges. However, these methods are often confined to settings (such as generative AI) where humans can interpret model outputs and provide feedback. In traditional non-generative settings, where model outputs are numerical values or classes, detecting misalignment through single-sample outputs is highly challenging.

In this paper we consider an alternative strategy. We propose interpreting model alignment through property testing, defining an aligned model f as one belonging to a subset \mathcal{P} of functions that exhibit specific desired behaviors. We focus on post-processing a pre-trained model f to better align with \mathcal{P} using conformal risk control. Specifically, we develop a general procedure for converting queries for a given property \mathcal{P} to a collection of loss functions suitable for use in a conformal risk control algorithm. We prove a probabilistic guarantee that the resulting conformal interval around f contains a function approximately satisfying \mathcal{P} .

Moreover, given the remarkable capabilities of modern AI models with large parameters and extensive training data, one might argue that alignment problems will naturally resolve, making alignment techniques unnecessary. However, we show that increasing the size of the training data or the number of parameters in a random feature model does not eliminate the need for alignment techniques when the pre-training data contains biased labels. We exhibit applications of our alignment methodology on a collection of supervised learning datasets for (shape-constrained) properties such as monotonicity and concavity. The general procedure is flexible and can be applied to a wide range of desired properties.

*Email: woverman@stanford.edu

†Email: jjvallon@alumni.stanford.edu

‡Email: bayati@stanford.edu

1 Introduction

The emergence of large foundation models has heightened the focus on the problem of alignment. Aligned models are artificial intelligences designed to pursue goals that align with human values, principles, and intentions [Leike et al., 2018, Ouyang et al., 2022, Hendrycks et al., 2023, Ngo et al., 2024]. Although the alignment problem is predominantly examined in the context of potential artificial general intelligence (AGI), large language models (LLMs), and reinforcement learning (RL) agents, it also has roots in the modern machine learning pipeline [D’Amour et al., 2022]. Motivated by this, we introduce a broader notion of alignment in this paper, extending beyond the aforementioned generative models to include even tabular regression models.

As an example, consider a regression task where \mathcal{P} represents models that are monotonically decreasing in a given feature. Constraining a prediction model during training to maintain monotonicity in this feature can be viewed as a form of alignment. However, ensuring that the predictions of a pre-trained model f are monotonically decreasing in this feature can be more complex. This complexity arises particularly in non-generative settings where the user cannot update a pre-trained f or obtain any outputs other than point predictions $f(X)$ for a given input X .

In this work, we propose an approach to this problem of aligning a pre-trained model f that is inspired by property testing [Ron, 2008, Goldreich, 2017] and utilizes conformal risk control [Angelopoulos et al., 2024]. We propose a definition of functions that either satisfy a property \mathcal{P} or are significantly far from satisfying \mathcal{P} , drawn from the field of property testing [Ron, 2008, Goldreich, 2017]. Property testing focuses on designing testing algorithms for determining membership to \mathcal{P} that are more efficient than the corresponding learning algorithms for \mathcal{P} [Ron, 2008]. From the perspective of modern deep learning models, we can imagine a user who wishes to determine whether a pre-trained model f belongs to \mathcal{P} but is unable to train a model of f ’s size.

Property testing algorithms generally perform local queries to determine, with high probability, whether a function has a given global property or is far from having that property. In this work, we consider mapping such queries for a given property of interest \mathcal{P} to a corresponding set of loss functions. These loss functions can then be used in a conformal risk control procedure [Angelopoulos et al., 2024] to obtain a notion of alignment for \mathcal{P} . In particular, we prove that running this procedure results in a conformal interval around f that contains a function close to \mathcal{P} .

We demonstrate our methodology on real-world datasets for the properties of monotonicity and concavity. To obtain asymmetric conformal intervals around f we provide a straightforward generalization of the results of Angelopoulos et al. [2024] to multi-dimensional $\lambda \in \mathbb{R}_{\geq 0}^k$. We focus the bulk of our experiments on monotonicity for the sake of exposition and because monotonicity constraints have been shown to be useful in promoting crucial aspects of alignment to human values, such as fairness and adherence to social norms [Wang and Gupta, 2020].

Given the outstanding capabilities of modern AI models with substantially large numbers of parameters and training data, one may argue that the alignment problem may naturally disappear as such advances continue [Kaplan et al., 2020], rendering alignment techniques such as those presented in this paper unnecessary. However, another contribution of this

paper is to refute this argument in a stylized setting, building on recent advances in the theory of linearized neural networks [Mei and Montanari, Misiakiewicz and Montanari, 2023]. Specifically, we show that increasing the size of the training data or the number of parameters in a random feature model cannot help it satisfy a property \mathcal{P} , if the pre-training data has biased labels. Our simulations show that the result holds even if only a small fraction of the training labels are impacted by the bias.

Summarizing our main contributions, we: (1) introduce an alignment perspective based on property testing, (2) use conformal risk control to post-process predictions of pre-trained models for better alignment, (3) generalize conformal risk control to multi-dimensional λ , and (4) demonstrate that increasing training data and parameters in a random feature model does not eliminate the need for alignment. We discuss related work in Section 6, particularly our connections to Yadkori et al. [2024], who use conformal risk control to address LLM hallucinations [Ji et al., 2023].

2 Preliminaries

In this section we provide condensed overviews of property testing and conformal prediction and risk control. The main definitions and concepts we will use from property testing are ε -farness and proximity oblivious testers (POTs). We also discuss one-sided testers, but primarily to motivate these former two definitions; our proposed alignment procedure will mainly rely on the definition of proximity oblivious testers. We also discuss conformal prediction, mainly focusing on conformal risk control, as this will be the main tool used to achieve alignment in our setting.

2.1 Properties and property testing

Our perspective on alignment in this work is motivated by the field of property testing [Ron, 2008, Goldreich, 2017]. The seminal work in this field by Blum et al. [1993] studied linearity testing of Boolean functions $f : \{0, 1\}^n \rightarrow \{0, 1\}$, and since then, there has been significant work on algorithms that are sublinear in n for querying properties \mathcal{P} such as low-degree polynomials [Kaufman and Ron, 2006, Bhattacharyya et al., 2009] and k -juntas [Blais, 2009]. In this spirit, property testing algorithms generally make local queries to a small part of a large object, such as a function or graph. From these sublinear number of queries, the algorithm attempts to determine whether the object has the property at a global level or is significantly far from having the property.

Definition 1 (ε -farness). *For a function $f : \mathcal{X} \rightarrow \mathcal{Y}$, a distribution \mathcal{D} over \mathcal{X} , $\varepsilon > 0$, and a property \mathcal{P} , we say f is ε -**far** from \mathcal{P} with respect to \mathcal{D} if $\delta_{\mathcal{P}, \mathcal{D}}(f) > \varepsilon$, where*

$$\delta_{\mathcal{P}, \mathcal{D}}(f) \stackrel{\text{def}}{=} \min_{g \in \mathcal{P}} \delta_{\mathcal{D}}(f, g) \quad \text{and} \quad \delta_{\mathcal{D}}(f, g) \stackrel{\text{def}}{=} \Pr_{x \sim \mathcal{D}} [f(X) \neq g(X)].$$

That is, any function $g \in \mathcal{P}$ agrees with f on inputs from \mathcal{D} with probability at most $1 - \varepsilon$ [Goldreich, 2017]. While property testing often assumes \mathcal{D} to be the uniform distribution, we will keep \mathcal{D} general, referred to as the *distribution-free* setting [Halevy and Kushilevitz, 2007], as we are concerned with queries over arbitrary calibration data distributions.

Following the definition introduced by [Halevy and Kushilevitz \[2007\]](#), a distribution-free **one-sided error tester** for a property \mathcal{P} is a probabilistic oracle machine M , which is provided with a distance parameter $\varepsilon > 0$, oracle access to an arbitrary function $f : \mathcal{X} \rightarrow \mathcal{Y}$, and oracle access to samples from a fixed but unknown distribution \mathcal{D} over \mathcal{X} , and satisfies the following two conditions:

1. If f satisfies \mathcal{P} , then $\Pr\{M^{f,\mathcal{D}} = \text{Accept}\} = 1$.
2. If f is ε -far from \mathcal{P} with respect to \mathcal{D} , then $\Pr\{M^{f,\mathcal{D}} = \text{Accept}\} \leq \frac{1}{3}$.

2.1.1 Proximity oblivious testers

Given the definition of testers above, it is natural to expect that any reasonable tester must take in ε as input. Many testing algorithms, however, rely on ε only for the sake of determining the appropriate number of times some basic test should be invoked [[Goldreich and Ron, 2008](#)]. The basic test itself does not use ε , so such basic tests are referred to as *proximity oblivious* [[Goldreich and Ron, 2008](#)].

Following [Goldreich and Ron \[2008\]](#), a *proximity-oblivious tester* (POT) for \mathcal{P} is a probabilistic oracle machine T that satisfies the following two conditions:

1. If f satisfies \mathcal{P} , then $\Pr\{T^{f,\mathcal{D}} = \text{Accept}\} = 1$.
2. There exists a monotone function $\rho : (0, 1] \rightarrow (0, 1]$ such that if $f \notin \mathcal{P}$, then $\Pr\{T^{f,\mathcal{D}} = \text{Reject}\} \geq \rho(\delta_{\mathcal{P},\mathcal{D}}(f))$.

The function ρ represents the detection probability of the tester T . Then we can obtain a one-sided error tester with parameter ε by simply making $\Theta(1/\rho(\varepsilon))$ calls to the POT T and accepting if and only if all the calls return `Accept` [[Goldreich and Ron, 2008](#)].

For example, consider the BLR test [[Blum et al., 1993](#)] over the boolean hypercube $\mathcal{X} = \{0, 1\}^n$, where the underlying distribution \mathcal{D} is uniform. This is a one-sided error tester that uses ε only to determine the number of calls it makes to a proximity oblivious tester. The POT $T^{f,\mathcal{D}}$ is the machine that samples $X_1, X_2 \sim \mathcal{D}$ and then checks whether $f(X_1) + f(X_2) = f(X_1 + X_2)$ or not. Clearly if f is indeed linear, then $\Pr\{T^{f,\mathcal{D}} = \text{Accept}\} = 1$, while if f is sufficiently far from \mathcal{P} , then there will be some nonzero probability of rejection by this tester [[Goldreich, 2017](#)].

2.2 Conformal prediction and conformal risk control

Our main tool for achieving alignment from this property perspective is built on conformal prediction and conformal risk control [[Vovk et al., 2005](#), [Bates et al., 2021](#), [Angelopoulos et al., 2024](#)]. Conformal prediction post-processes the outputs of any model f to create prediction intervals $C(\cdot)$ that ensure certain statistical coverage guarantees. Using a calibration dataset $\{(X_i, Y_i)\}_{i=1}^n$ consisting of ground truth input-output pairs, conformal prediction constructs intervals around the predictions of f such that $\Pr[Y_{n+1} \notin C(X_{n+1})] \leq \alpha$ for a user-specified error rate α on a test point (X_{n+1}, Y_{n+1}) .

This guarantee is notably distribution-free and holds for any function f . The probability is over the randomness in all $n + 1$ points; both the calibration set and the test point. The construction of $C(\cdot)$ depends on both the model f and the draw of the calibration data.

The conformal risk control framework extends conformal prediction to notions of error beyond miscoverage [Angelopoulos et al., 2024]. Given an exchangeable collection of non-increasing, random loss functions $L_i : \Lambda \rightarrow (-\infty, B]$, $i = 1, \dots, n + 1$, conformal risk control uses the first n loss functions and calibration data $\{(X_i, Y_i)\}_{i=1}^n$ to determine $\hat{\lambda}$ such that

$$\mathbb{E}[L_{n+1}(\hat{\lambda})] \leq \alpha.$$

Consider loss functions of the form $L_i(\lambda) = \ell(C_\lambda(X_i), Y_i)$, where $C_\lambda(X_i)$ is a set of outputs constructed by f and the calibration data. Larger values of λ generate more conservative prediction sets $C_\lambda(\cdot)$. Let the risk on the calibration data for a given λ be $\hat{R}_n(\lambda) = \frac{1}{n} \sum_{i=1}^n L_i(\lambda)$. For a user-specified risk rate α , we let

$$\hat{\lambda} = \inf \left\{ \lambda : \frac{n}{n+1} \hat{R}_n(\lambda) + \frac{B}{n+1} \leq \alpha \right\}.$$

This choice of $\hat{\lambda}$ guarantees the desired risk control $\mathbb{E}[L_{n+1}(\hat{\lambda})] \leq \alpha$ [Angelopoulos et al., 2024].

3 Conformal property alignment

Our main methodology is to use conformal risk control to create prediction intervals that align with specific properties \mathcal{P} . Our approach allows us to post-process the outputs of a pre-trained model f to ensure that within the resulting conformal band, with a given probability, there exists predictions that adhere to desired properties such as monotonicity. We first present a generalization of conformal risk control [Angelopoulos et al., 2024] that extends to multi-dimensional λ .

3.1 Multi-lambda conformal risk control

We generalize the conformal risk control algorithm to a k -dimensional vector of lambda values $\lambda = (\lambda_1, \lambda_2, \dots, \lambda_k)$, where larger $\lambda \in \mathbb{R}^k$ yield more conservative outputs. The construction of $C_\lambda(X_i)$ depends on the application and allows for flexibility in the use of $f(X_i)$ and λ .

Definition 2 ($C_\lambda(X)$ and $C_\lambda(f)$). *For each point $X_i \in \mathcal{X}$, define $C_\lambda(X_i)$ as the conformal set of predictions for X_i constructed from f and λ . Then, $C_\lambda(f)$ is the conformal interval around f that includes $C_\lambda(X_i)$ for every $X_i \in \mathcal{X}$.*

Following the original scalar λ setting [Angelopoulos et al., 2024], we assess C_λ using non-increasing random loss functions $L_i = \ell(C_\lambda(X_i), Y_i) \in (-\infty, B]$ for $B < \infty$. In particular, we consider an exchangeable collection of non-increasing random functions $L_i : \Lambda \rightarrow (-\infty, B]$, $i = 1, \dots, n + 1$, where $\Lambda \subset \mathbb{R}_{\geq 0}^k$ is a bounded subset of $\mathbb{R}_{\geq 0}^k$, with bound λ_j^{\max} in each dimension $j \in [k]$.

As in Angelopoulos et al. [2024], we use the first n functions to determine $\hat{\lambda}$ so that the risk on the $(n + 1)$ -th function is controlled, specifically so that $\mathbb{E}[L_{n+1}(\hat{\lambda})] \leq \alpha$.

We apply a similar algorithm. Given $\alpha \in (0, B)$ and letting $\hat{R}_n(\lambda) = \frac{L_1(\lambda) + \dots + L_n(\lambda)}{n}$, define

$$\Lambda_{\min} = \text{Min} \left\{ \boldsymbol{\lambda} : \frac{n}{n+1} \hat{R}_n(\boldsymbol{\lambda}) + \frac{B}{n+1} \leq \alpha \right\}$$

to be the set of minimal elements [Boyd and Vandenberghe, 2004] of Λ that satisfy the condition $\frac{n}{n+1} \hat{R}_n(\boldsymbol{\lambda}) + \frac{B}{n+1} \leq \alpha$. Let $g : \Lambda \rightarrow \mathbb{R}$ be a strictly increasing function with respect to the product order on \mathbb{R}^k . Thus each $L_i(\boldsymbol{\lambda})$ is non-increasing with respect to the level sets defined by $g(\boldsymbol{\lambda})$. Then select $\hat{\boldsymbol{\lambda}} \in \Lambda_{\min}$ to be a minimizer of g over Λ_{\min} .

We then deploy the resulting conformal band $C_{\hat{\boldsymbol{\lambda}}}$ on the test point X_{n+1} . For this choice of $\hat{\boldsymbol{\lambda}}$, we have a risk control guarantee that mimics the result of Angelopoulos et al. [2024], specifically:

Proposition 1. *Assume that $L_i(\boldsymbol{\lambda})$ is non-increasing with respect to the partial ordering of Λ inherited from the product order on \mathbb{R}^k . Additionally let $g(\boldsymbol{\lambda})$ be a strictly increasing function $g : \Lambda \rightarrow \mathbb{R}$. Also assume L_i is right-continuous in each dimension, $L_i(\boldsymbol{\lambda}^{\max}) \leq \alpha$, and $\sup_{\boldsymbol{\lambda}} L_i(\boldsymbol{\lambda}) \leq B < \infty$ almost surely. Then*

$$\mathbb{E}[L_{n+1}(\hat{\boldsymbol{\lambda}})] \leq \alpha.$$

The proof is similar to the proof of the guarantee for the conformal risk control algorithm in Angelopoulos et al. [2024] and is deferred to Appendix A.

To provide intuition on $g(\boldsymbol{\lambda})$, we note that for our primary use case we will take $g(\boldsymbol{\lambda}) = \sum_{i=1}^k \lambda_i$. Clearly this function is strictly increasing in $\boldsymbol{\lambda}$ and intuitively it is reasonable to consider loss functions L_i that are non-increasing as the sum of the components of $\boldsymbol{\lambda}$ increases.

3.2 Conformal property alignment from proximity oblivious testers

Now we show how to construct a conformal risk control problem from proximity oblivious testers for a given property \mathcal{P} . Let $\mathbb{T}(f, X, Y)$ be the random output of $\mathbb{T}^{f, \mathcal{D}}$ evaluated at $(X, Y) \sim D$. Note there can be randomness in the machine besides sampling $(X, Y) \sim D$, and each individual loss function will be defined with respect to fixing this randomness:

Definition 3 ($C_{\boldsymbol{\lambda}}(\mathbb{T})$). *We set $L_i = \ell(C_{\boldsymbol{\lambda}}(X_i), Y_i) = 0$ if after fixing the remaining randomness in \mathbb{T} , there exists \tilde{f} such that $\mathbb{T}(\tilde{f}, X_i, Y_i) = \text{Accept}$ where \tilde{f} is the function resulting from modifying f to take some value $\tilde{Y} \in C_{\boldsymbol{\lambda}}(X_i)$ at X_i . Otherwise, $L_i = \ell(C_{\boldsymbol{\lambda}}(X_i), Y_i) = 1$. Define the set of loss functions obtained from this mapping to be $C_{\boldsymbol{\lambda}}(\mathbb{T})$.*

Intuitively, the POT may fail for the original value of the function $f(X_i)$ at X_i , but if we can adjust the value of f to take some value \tilde{Y} that falls within $C_{\boldsymbol{\lambda}}(X_i)$ such that the function now satisfies the query at point X_i , then we take the loss to be zero. We use conformal risk control to find a $\boldsymbol{\lambda}$ such that with a sufficiently high probability this loss will be zero at a random data point. The goal is not to obtain a specific new function, but rather a band around f for which we can establish probabilistic guarantees of predictions within the band satisfying \mathcal{P} as determined by \mathbb{T} .

Linearity example. Consider the BLR test mentioned in Section 2.1.1. We use a 2 dimensional $\lambda = (\lambda^-, \lambda^+)$ to generate $C_\lambda(X_i) = [f(X_i) - \lambda^-, f(X_i) + \lambda^+]$. Now the POT \mathbb{T} for linearity samples $(X_1, Y_1) \sim \mathcal{D}$ and then uses the rest of its randomness to sample $X_2 \sim \text{Unif}(\mathcal{X})$. We have $L_1 = \ell(C_\lambda(X_1), Y_1) = 0$ if there exists an output $\tilde{f}(X_1) \in [f(X_1) - \lambda^-, f(X_1) + \lambda^+]$ such that $\tilde{f}(X_1) = f(X_1 + X_2) - f(X_2)$, and $L_1 = \ell(C_\lambda(X_1), Y_1) = 1$ otherwise. Intuitively, we set the loss to 0 if there is some output $\tilde{Y} \in [f(X_1) - \lambda^-, f(X_1) + \lambda^+]$ such that f taking that value would satisfy linearity with respect to X_2 .

Note that in this case the tester and loss function does not depend on the Y_i . This is because the property of f being monotone does not depend on the Y_i and here \mathcal{D} is only used to obtain samples of the X_i . This is not the case in general, however, and properties can be defined with respect to the whole sample $(X_i, Y_i) \sim \mathcal{D}$. For example, we could consider the property \mathcal{P} that f does not over-predict, that is, for $(X, Y) \sim \mathcal{D}$ we have $f(X) \leq Y$. Now we state our main theorem.

Theorem 1. *If we run conformal risk control on a calibration dataset $\{(X_i, Y_i)\}_{i=1}^n$ from a distribution \mathcal{D} using parameter α and loss functions $L = C_\lambda(\mathbb{T})$ mapped from a proximity oblivious tester \mathbb{T} for property \mathcal{P} , then with probability at least $1 - \alpha$ there exists a function $\tilde{f} \in C_{\hat{\lambda}}(f)$ such that \tilde{f} is at most α -far from \mathcal{P} with respect to \mathcal{D} .*

Proof. Conformal risk control guarantees us that $\mathbb{E}[L_{n+1}(C_{\hat{\lambda}}(X_{n+1}), Y_{n+1})] \leq \alpha$. Note that the randomness in this expectation is over the randomness in all of the $n + 1$ points. We have

$$\begin{aligned} \alpha &\geq \mathbb{E}[L_{n+1}(C_{\hat{\lambda}}(X_{n+1}), Y_{n+1})] \\ \alpha &\geq \Pr_{(X_1, Y_1), \dots, (X_{n+1}, Y_{n+1}) \sim \mathcal{D}} [\forall \tilde{f} \in C_{\hat{\lambda}}(f), \mathbb{T}(\tilde{f}, X_{n+1}, Y_{n+1}) = \text{Reject}] \\ 1 - \alpha &\leq \Pr_{(X_1, Y_1), \dots, (X_{n+1}, Y_{n+1}) \sim \mathcal{D}} [\exists \tilde{f} \in C_{\hat{\lambda}}(f), \mathbb{T}(\tilde{f}, X_{n+1}, Y_{n+1}) = \text{Accept}] \\ 1 - \alpha &\leq \Pr_{(X_{n+1}, Y_{n+1}) \sim \mathcal{D}} [\exists \tilde{f} \in C_{\hat{\lambda}}(f), \mathbb{T}(\tilde{f}, (X_{n+1}, Y_{n+1})) = \text{Accept} | \hat{\lambda}] \Pr_{(X_1, Y_1), \dots, (X_n, Y_n) \sim \mathcal{D}} [\hat{\lambda}] \end{aligned}$$

So with probability at least $1 - \alpha$ over the random draw of $(X_1, Y_1), \dots, (X_n, Y_n)$ we have that $\hat{\lambda}$ is such that with probability at least $1 - \alpha$ over sample $(X_{n+1}, Y_{n+1}) \sim \mathcal{D}$ we can find a point $\tilde{Y}_{n+1} \in C_{\hat{\lambda}}(X_{n+1})$ such that the POT \mathbb{T} accepts. For the points (X, Y) in the support of \mathcal{D} for which we can find such a $\tilde{Y} \in C_{\hat{\lambda}}(X)$, set $\tilde{f}(X) = \tilde{Y}$. Then define $\tilde{g}(X)$ to agree with $\tilde{f}(X)$ at these points and take a value such that \mathbb{T} accepts at other points in $\mathcal{X} \times \mathcal{Y}$. Thus $\tilde{g} \in \mathcal{P}$. Then we have that $\Pr_{(X, Y) \sim \mathcal{D}} [\tilde{f}(X) \neq \tilde{g}(X)] \leq \alpha$. So $\min_{g \in \mathcal{P}} \Pr_{(X, Y) \sim \mathcal{D}} [\tilde{f}(X) \neq g(X)] \leq \alpha$, hence \tilde{f} is at most α far from \mathcal{P} with respect to \mathcal{D} . \square

4 Examples

4.1 Monotonicity

Monotonic behavior is important in various applications. We focus on monotonicity in a single feature, where we expect that $f(X)$ should have monotonically increasing or decreasing behavior with respect to a certain feature x^k when other features x^{-k} are held fixed. While

there is a long-standing literature on using monotonic constraints for regularization [Brunk et al., 1973, Sill and Abu-Mostafa, 1996, You et al., 2017, Bonakdarpour et al., 2018] and on integrating such monotonic shape constraints into prediction models [Groeneboom and Jongbloed, 2014, Cano et al., 2018, Runje and Shankaranarayana, 2023], our aim is not to view monotonicity as a possible means to improve test accuracy, but rather as a user-desired property for safe or fair deployment of a given model. For example, Wang and Gupta [2020] highlight the importance of monotonicity in models for criminal sentencing, wages, and medical triage.

Consider a user given a pre-trained model f that was not trained with monotonic constraints. The user, however, wishes for the sake of safe or fair deployment to make predictions in a way that is as monotonic as possible. In particular, let \mathcal{P} be the property that f is monotonically decreasing in dimension k . To apply our methodology we consider the following proximity oblivious tester \mathbb{T} in Algorithm 1.

Algorithm 1 POT \mathbb{T} for monotonically decreasing in a fixed dimension k

- 1: Sample $(X_1, Y_1) \sim \mathcal{D}$. Let $X_1 = (x_1, x^{-k})$
 - 2: Sample x_2 uniformly from the range of dimension k . Set $X_2 = (x_2, x^{-k})$
 - 3: **if** $x_1 < x_2$ and $f(X_1) < f(X_2)$ **then**
 - 4: **return** Reject
 - 5: **else if** $x_2 < x_1$ and $f(X_2) < f(X_1)$ **then**
 - 6: **return** Reject
 - 7: **end if**
 - 8: **return** Accept
-

Clearly this tester will always return Accept when $f \in \mathcal{P}$, and if $\delta_{\mathcal{P}, \mathcal{D}}(f) > 0$, then there will be some nonzero probability that \mathbb{T} returns Reject. We apply our conformal property alignment from POT procedure to obtain loss functions $L_i = \ell(C_\lambda(X_i), Y_i)$. On our calibration set $\{(X_i, Y_i)\}_{i=1}^n$ we obtain a loss function L_i for each i that is obtained from fixing the randomness in \mathbb{T} to obtain a x_{i2} for each point i . Note that after fixing this randomness, since the calibration data point (X_i, Y_i) is also fixed, each loss function L_i becomes a deterministic function of λ .

Now according to our construction of the loss functions in Section 3.2, we have that $L_i = \ell(C_\lambda(X_{i1}), Y_i) = 0$ if there exists \tilde{f} such that, with the fixed randomness of sampling X_{i2} , we have $\mathbb{T}(\tilde{f}, X_{i1}) = \text{Accept}$, where \tilde{f} is the function resulting from modifying f to take some value $\tilde{Y} \in [f(X_{i1}) - \lambda^-, f(X_{i1}) + \lambda^+]$. Otherwise, $L_i = \ell(C_\lambda(X_{i1}), Y_i) = 1$. Intuitively, we have zero loss if we can find some point in the conformal band around $f(X_{i1})$ such that monotonicity (decreasing) is preserved with respect to X_{i2} in the sense that monotonicity POT \mathbb{T} returns Accept.

Setup. We align for monotonicity on various UCI ML repository datasets [Dua and Graff, 2023] with a 70-15-15 train-calibrate-test split, averaged over 10 random splits. We use XGBoost regression models [Chen and Guestrin, 2016]. For each dataset, we select a feature for which we desire the model to be monotonic, not with the intention of improving test-set accuracy, but from the perspective of a user who desires this property.

We train two models per dataset: one unconstrained, trained on the training set, and another constrained to be monotonic, trained on both the training and calibration sets. The conformal risk control procedure is applied to the unconstrained model using the calibration data. The constrained model can be considered best possible from the user’s perspective, using all available pre-test data and satisfying the monotonicity property \mathcal{P} during training.

To compare performance with respect to the training metric of accuracy, we convert conformal intervals into point predictions by taking k -quantiles of the constrained feature, linearly interpolating between adding λ^+ at the lowest quantile to subtracting λ^- at the highest quantile for monotonically decreasing, or vice versa for monotonically increasing.

Results. Table 1 presents results on the test set for the Combined Cycle Power Plant dataset [Tfekci and Kaya, 2014]. In practice, Exhaust-vacuum is known to negatively influence turbine efficiency [Tfekci and Kaya, 2014]. The conformal procedure outperforms the constrained model in terms of MSE for $\alpha = 0.1$ and $\alpha = 0.05$, but worsens for $\alpha = 0.01$. The risk metric closely matches the theoretical guarantee from conformal risk control and achieves optimal performance of 0 for the constrained model. Additional datasets and results are detailed in the appendix.

Table 1: Power Plant, $n = 9568$. Monotonically decreasing on Exhaust Vacuum. $\lambda^{\max} = (10, 10)$, $g(\lambda) = \lambda^+ + \lambda^-$.

α	λ	Metric	Unconstrained	Conformal	Constrained
0.1	$\lambda^+ = 0.96$	MSE	9.99	10.35	15.31
	$\lambda^- = 1.18$	Risk	0.17	0.111	0
0.05	$\lambda^+ = 1.94$	MSE	9.99	11.37	15.31
	$\lambda^- = 2.68$	Risk	0.17	0.058	0
0.01	$\lambda^+ = 4.76$	MSE	9.99	15.56	15.31
	$\lambda^- = 4.88$	Risk	0.17	0.012	0

4.2 Concavity

Concavity and convexity are crucial behaviors in many applications. In this context, we focus on concavity in a single feature. A common example where users might expect concave behavior is in recommendation or preference prediction models. According to economic theory, the utility function with respect to the quantity of an item is often quasi-concave, reflecting the principle of diminishing marginal utility [Mas-Colell et al., 1995]. Jenkins et al. [2021] propose a novel loss function to account for this expected concavity, which aligns the model with the concavity property \mathcal{P} during training. Here we again consider aligning a pre-trained model, not trained to satisfy \mathcal{P} , using a proximity oblivious tester T for \mathcal{P} as described in Algorithm 2.

In this case we use a scalar λ and have that that $L = \ell(C_\lambda(X), Y) = 0$ if $f(X) + \lambda \geq \frac{f(X_l) + f(X_r)}{2}$, and $L = \ell(C_\lambda(X), Y) = 1$ otherwise. We demonstrate running conformal risk control with this loss function on a real-world dataset in the appendix.

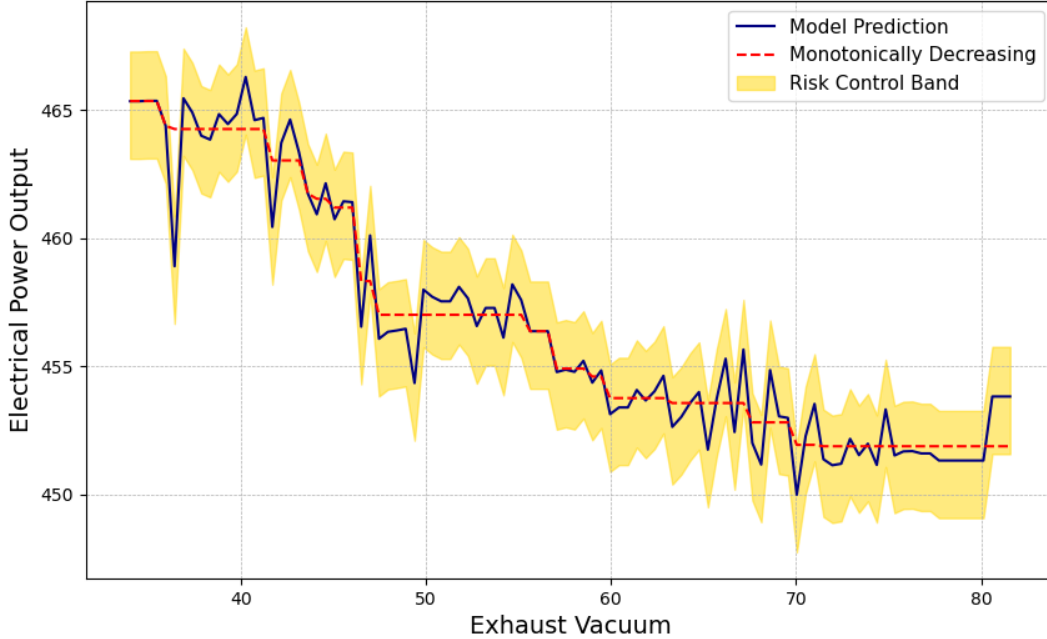


Figure 1: Univariate partial dependence plot of unconstrained model. Risk control band for $\alpha = 0.05$. Dashed line exemplifying Theorem 1 demonstrating existence of monotonically decreasing function falling within the conformal band on $0.97 > 1 - \alpha$ fraction of the domain.

5 A stylized examination of alignment persistence in AI models

Consider data generated as:

$$y = g(X) + h(X) + \varepsilon,$$

where ε is mean-zero noise with variance τ^2 independent of X . Here, $h(X)$ is biased noise we want to ignore, aiming to learn only $g(X)$. Consider the case in which experts expect data to follow $g(X) + \text{unbiased noise}$, but biased noise $h(X)$ can obscure this.

One potential reason for the presence of biased noise in data could be due to a measurement error of the outcome that is correlated with select features, leading to an incorrectly calculated outcome. A biased measurement error could occur if there is incomplete data and the presence of the incomplete data is correlated with select features in an unexpected, systematic way. Our goal is to understand how this bias affects model behavior when trying to learn $g(X)$ alone.

Given n i.i.d. samples $\{(X_i, Y_i)\}_{i=1}^n$ from the above model, we denote this dataset by \mathcal{D}_n . We use a random feature model:

$$f_{\text{RF}}(X; \mathbf{a}, \{\mathbf{w}_j\}_{j \in [N]}) = \frac{1}{\sqrt{N}} \sum_{j \in [N]} a_j \sigma(\langle X, \mathbf{w}_j \rangle),$$

Algorithm 2 POT T for concavity in a fixed dimension k

- 1: Sample $(X, Y) \sim \mathcal{D}$. Let $X = (x, x^{-k})$
 - 2: Let L and R be the subset of points in dimension k less than x and greater than x , respectively.
 - 3: Sample x_l uniformly from L and x_r uniformly from R .
 - 4: Set $X_l = (x_l, x^{-k}), X_r = (x_r, x^{-k})$
 - 5: **if** $f(X) < \frac{f(X_l)+f(X_r)}{2}$ **then**
 - 6: **return** Reject
 - 7: **end if**
 - 8: **return** Accept
-

where $\mathbf{a} \in \mathbb{R}^N$ are learned weights, and $\{\mathbf{w}_j\}_{j \in [N]}$ are fixed random weights. The squared loss is minimized by ridge regression:

$$\hat{\mathbf{a}}_\lambda = \arg \min_{\mathbf{a} \in \mathbb{R}^N} \sum_{i \in [n]} (Y_i - f_{\text{RF}}(X_i))^2 + \lambda \|\mathbf{a}\|_2^2.$$

Users expect a model to exhibit a property \mathcal{P} , satisfied by $g(X)$ but not necessarily by $g(X) + h(X)$. We can constrain training to ensure \mathcal{P} . Let $C_{\mathcal{P}} = \{\mathbf{a} \mid \mathbf{a} \in \mathbb{R}^N \text{ and } f_{\text{RF}}(X; \mathbf{a}) \text{ satisfies } \mathcal{P}\}$, yielding a constrained model: $\hat{\mathbf{a}}_{\lambda, \mathcal{P}} = \arg \min_{\mathbf{a} \in C_{\mathcal{P}}} \sum_{i \in [n]} (Y_i - f_{\text{RF}}(X_i))^2 + \lambda \|\mathbf{a}\|_2^2$.

Assuming g and h are polynomials with $\deg_g < \deg_h$, and given specific conditions on data size and model parameters, we consider two settings: (i) *Classic*: $d^{\deg_g + \delta} < N < d^{\deg_h - \delta}$, and (ii) *Underspecified*: $N > d^{\deg_h + \delta}$ for a small $\delta > 0$.

In Appendix C, we utilize results from Misiakiewicz and Montanari [2023] to derive insights into the impact of model complexity and data size on adherence to \mathcal{P} . In particular, we show that under certain assumptions, including small noise bias and robustness of property \mathcal{P} , the constrained and unconstrained models have zero distance in the classic setting: $\hat{\mathbf{a}}_{\lambda, \mathcal{P}} = \hat{\mathbf{a}}_\lambda$. However, in the underspecified setting, the constrained and unconstrained models will differ, resulting in a non-zero distance: $\hat{\mathbf{a}}_{\lambda, \mathcal{P}} \neq \hat{\mathbf{a}}_\lambda$. This result implies that in the presence of noise bias, the overparameterized models (i.e., underspecified setting) fail to satisfy the property \mathcal{P} , and this cannot be remedied as the data size increases.

6 Related work

Our paper draws from a broad range of areas, hence we refer the reader to textbooks and surveys in alignment [Everitt et al., 2018, Hendrycks et al., 2022, Ji et al., 2024, Hendrycks, 2024], conformal prediction [Angelopoulos and Bates, 2022], property testing [Ron, 2008, Goldreich, 2017], and linearized neural networks [Misiakiewicz and Montanari, 2023].

RLHF [Christiano et al., 2017] has been notably effective in aligning LLMs with human values and intentions, as demonstrated by [Ouyang et al., 2022]. Our work considers attempts at alignment that generalizes to models without human-interpretable outputs, which has connections to the scalable oversight problem [Irving et al., 2018, Christiano et al., 2018, Wu et al., 2021]. Goal misgeneralization [Langosco et al., 2022, Shah et al., 2022] has potential connections to the underspecified pipeline [D’Amour et al., 2022] considered in this paper

in the sense that models with equivalent performance according to the training metric may differ in some other user-desired property during deployment. One of the main methods of assurance [Batarseh et al., 2021], which is concerned with assessing the alignment of pre-trained AI systems, is safety evaluations [Perez et al., 2022, Shevlane et al., 2023] meant to assess risk during deployment, which also has connections to our approach.

Connections to Yadkori et al. [2024]. The work of Yadkori et al. [2024] closely aligns with ours in both methodology and theme, utilizing conformal risk control to reduce LLM hallucinations [Ji et al., 2023]. To demonstrate our framework’s flexibility and generality, we apply it to their context. They examine a potentially random LLM $f : \mathcal{X} \rightarrow \mathcal{Y}$ and assume access to a confidence score function $g : \mathcal{X} \rightarrow \mathbb{R}$. They use an abstention function $a : \Lambda \times \mathcal{X} \rightarrow \{0, 1\}$ that decides whether the model should abstain from answering where $a_\lambda(X) = 1$ if $g(X) < \lambda$ and $a_\lambda(X) = 0$ if $g(X) \geq \lambda$. The match function $m : \mathcal{X} \times \mathcal{Y} \times \mathcal{Y} \rightarrow \{0, 1\}$ is used to determine if a response Y' is semantically equivalent to Y , indicating hallucination if not.

Yadkori et al. [2024] use conformal risk control to find an optimal $\hat{\lambda}$ such that the pair $(a_{\hat{\lambda}}, f)$ hallucinates at a rate less than α . The loss function they use is $\ell : \mathcal{X} \times \mathcal{Y} \times \Lambda \rightarrow \mathbb{R}$ such that ℓ punishes failure to abstain when the response does not match the label, that is

$$\ell(X, Y; \lambda) = (1 - a_\lambda(X))(1 - m(X; f(X), Y)). \quad (1)$$

In this case we do not change the outputs of the function f itself, instead we use conformal risk control to change the outputs of a . Consider the property \mathcal{P} to be that (a, f) does not hallucinate. A tester for \mathcal{P} is then simply to query (a, f) on some input X and Reject if f hallucinates or Accept otherwise. Now when $g(X) < \lambda$, we have $C_\lambda(X) = \{f(X), \text{Abstain}\}$ meaning that (a, f) can avoid hallucinating, so the tester will Accept.

Yadkori et al. [2024] use a separate conformal procedures for setting λ and a parameter β with which they define $m(X; Y', Y) = \mathbb{I}(s(X; Y', Y) \geq \beta)$, where the similarity function $s : \mathcal{X} \times \mathcal{Y} \times \mathcal{Y} \rightarrow \mathbb{R}$ is assumed to be given. We can use our multi-lambda conformal risk control with $\boldsymbol{\lambda} = (\lambda_a, \lambda_m)$ to set these parameters simultaneously using a single calibration set $\{(X_i, Y_i)\}_{i=1}^n$ of ground truth query-response pairs sampled from the true data distribution \mathcal{D} . Let

$$\ell(X, Y; \boldsymbol{\lambda}) = (1 - a_{\lambda_a}(X))(1 - \mathbb{I}(s(X; f(X), Y) \geq 1 - \lambda_m))$$

Then we can take $g(\boldsymbol{\lambda}) = c_1\lambda_a + c_2\lambda_m$ for $c_1, c_2 \geq 0$ and choose $\boldsymbol{\lambda}$ by our multi-lambda conformal risk control procedure. As required, this loss function is non-increasing with respect to $\boldsymbol{\Lambda}$ and $g(\boldsymbol{\lambda})$.

7 Discussion

We introduce a method to align pre-trained models with desired user properties using conformal risk control. By post-processing outputs using property dependent loss functions, we provide probabilistic guarantees that conformal intervals contain functions close to the

desired set. This allows for alignment without retraining, effective in both generative and non-generative contexts. Future work should extend these techniques to more properties, explore sample complexity and adaptive querying, and potentially apply them to policy functions in MPD settings for RL agent safety guarantees.

References

- Anastasios N. Angelopoulos and Stephen Bates. A gentle introduction to conformal prediction and distribution-free uncertainty quantification, 2022.
- Anastasios Nikolas Angelopoulos, Stephen Bates, Adam Fisch, Lihua Lei, and Tal Schuster. Conformal risk control. In *The Twelfth International Conference on Learning Representations*, 2024.
- Feras A. Batarseh, Laura Freeman, and Chih-Hao Huang. A survey on artificial intelligence assurance. *Journal of Big Data*, 8(1), April 2021. ISSN 2196-1115. doi: 10.1186/s40537-021-00445-7. URL <http://dx.doi.org/10.1186/s40537-021-00445-7>.
- Stephen Bates, Anastasios Angelopoulos, Lihua Lei, Jitendra Malik, and Michael I. Jordan. Distribution-free, risk-controlling prediction sets, 2021.
- Arnab Bhattacharyya, Swastik Kopparty, Grant Robert Schoenebeck, Madhu Sudan, and David Zuckerman. Optimal testing of reed-muller codes. *2010 IEEE 51st Annual Symposium on Foundations of Computer Science*, pages 488–497, 2009. URL <https://api.semanticscholar.org/CorpusID:25924>.
- Eric Blais. Testing juntas nearly optimally. pages 151–158, 05 2009. doi: 10.1145/1536414.1536437.
- Manuel Blum, Michael Luby, and Ronitt Rubinfeld. Self-testing/correcting with applications to numerical problems. *Journal of Computer and System Sciences*, 47(3):549–595, 1993. ISSN 0022-0000. doi: [https://doi.org/10.1016/0022-0000\(93\)90044-W](https://doi.org/10.1016/0022-0000(93)90044-W). URL <https://www.sciencedirect.com/science/article/pii/002200009390044W>.
- Matt Bonakdarpour, Sabyasachi Chatterjee, Rina Foygel Barber, and John Lafferty. Prediction rule reshaping, 2018.
- Stephen Boyd and Lieven Vandenberghe. *Convex optimization*. Cambridge university press, 2004.
- Hugh D. Brunk, Richard E. Barlow, David J. Bartholomew, and Joan M. Bremner. Statistical inference under order restrictions : the theory and application of isotonic regression. *International Statistical Review*, 41:395, 1973. URL <https://api.semanticscholar.org/CorpusID:120349543>.
- José-Ramón Cano, Pedro Antonio Gutiérrez, Bartosz Krawczyk, Michał Woźniak, and Salvador García. Monotonic classification: an overview on algorithms, performance measures and data sets, 2018.

- Tianqi Chen and Carlos Guestrin. Xgboost: A scalable tree boosting system. In *Proceedings of the 22nd ACM SIGKDD International Conference on Knowledge Discovery and Data Mining*, KDD '16. ACM, August 2016. doi: 10.1145/2939672.2939785. URL <http://dx.doi.org/10.1145/2939672.2939785>.
- Paul Christiano, Buck Shlegeris, and Dario Amodei. Supervising strong learners by amplifying weak experts, 2018.
- Paul F Christiano, Jan Leike, Tom Brown, Miljan Martic, Shane Legg, and Dario Amodei. Deep reinforcement learning from human preferences. In I. Guyon, U. Von Luxburg, S. Bengio, H. Wallach, R. Fergus, S. Vishwanathan, and R. Garnett, editors, *Advances in Neural Information Processing Systems*, volume 30. Curran Associates, Inc., 2017. URL https://proceedings.neurips.cc/paper_files/paper/2017/file/d5e2c0adad503c91f91df240d0cd4e49-Paper.pdf.
- Alexander D'Amour, Katherine Heller, Dan Moldovan, Ben Adlam, Babak Alipanahi, Alex Beutel, Christina Chen, Jonathan Deaton, Jacob Eisenstein, Matthew D. Hoffman, Farhad Hormozdiari, Neil Houlsby, Shaobo Hou, Ghassen Jerfel, Alan Karthikesalingam, Mario Lucic, Yian Ma, Cory McLean, Diana Mincu, Akinori Mitani, Andrea Montanari, Zachary Nado, Vivek Natarajan, Christopher Nielson, Thomas F. Osborne, Rajiv Raman, Kim Ramasamy, Rory Sayres, Jessica Schrouff, Martin Seneviratne, Shannon Sequeira, Harini Suresh, Victor Veitch, Max Vladymyrov, Xuezhi Wang, Kellie Webster, Steve Yadlowsky, Taedong Yun, Xiaohua Zhai, and D. Sculley. Underspecification presents challenges for credibility in modern machine learning. *Journal of Machine Learning Research*, 23(1), jan 2022. ISSN 1532-4435.
- Dheeru Dua and Casey Graff. Uci machine learning repository, 2023. URL <http://archive.ics.uci.edu/ml>.
- Tom Everitt, Gary Lea, and Marcus Hutter. Agi safety literature review, 2018.
- Oded Goldreich. *Introduction to Property Testing*. Cambridge University Press, 2017.
- Oded Goldreich and Dana Ron. On proximity-oblivious testing. *Electronic Colloquium on Computational Complexity (ECCC)*, 15, 01 2008. doi: 10.1137/100789646.
- Piet Groeneboom and Geurt Jongbloed. *Nonparametric Estimation under Shape Constraints: Estimators, Algorithms and Asymptotics*. Cambridge Series in Statistical and Probabilistic Mathematics. Cambridge University Press, Cambridge, 2014. ISBN 978-0-521-86401-5. doi: 10.1017/CBO9781139020893.
- Shirley Halevy and Eyal Kushilevitz. Distribution-free property-testing. *SIAM J. Comput.*, 37:1107–1138, 01 2007. doi: 10.1007/978-3-540-45198-3_26.
- Dan Hendrycks. *AI Safety, Ethics, and Society*. Center for AI Safety, 2024. URL <https://www.aisafetybook.com/>.
- Dan Hendrycks, Nicholas Carlini, John Schulman, and Jacob Steinhardt. Unsolved problems in ml safety, 2022.

- Dan Hendrycks, Collin Burns, Steven Basart, Andrew Critch, Jerry Li, Dawn Song, and Jacob Steinhardt. Aligning ai with shared human values, 2023.
- Geoffrey Irving, Paul Christiano, and Dario Amodei. Ai safety via debate, 2018.
- Porter Jenkins, Ahmad Farag, J. Stockton Jenkins, Huaxiu Yao, Suhang Wang, and Zhenhui Li. Neural utility functions. *Proceedings of the AAAI Conference on Artificial Intelligence*, 35(9):7917–7925, May 2021. doi: 10.1609/aaai.v35i9.16966. URL <https://ojs.aaai.org/index.php/AAAI/article/view/16966>.
- Jiaming Ji, Tianyi Qiu, Boyuan Chen, Borong Zhang, Hantao Lou, Kaile Wang, Yawen Duan, Zhonghao He, Jiayi Zhou, Zhaowei Zhang, Fanzhi Zeng, Kwan Yee Ng, Juntao Dai, Xuehai Pan, Aidan O’Gara, Yingshan Lei, Hua Xu, Brian Tse, Jie Fu, Stephen McAleer, Yaodong Yang, Yizhou Wang, Song-Chun Zhu, Yike Guo, and Wen Gao. Ai alignment: A comprehensive survey, 2024.
- Ziwei Ji, Nayeon Lee, Rita Frieske, Tiezheng Yu, Dan Su, Yan Xu, Etsuko Ishii, Ye Jin Bang, Andrea Madotto, and Pascale Fung. Survey of hallucination in natural language generation. *ACM Computing Surveys*, 55(12):1–38, March 2023. ISSN 1557-7341. doi: 10.1145/3571730. URL <http://dx.doi.org/10.1145/3571730>.
- Jared Kaplan, Sam McCandlish, Tom Henighan, Tom B. Brown, Benjamin Chess, Rewon Child, Scott Gray, Alec Radford, Jeffrey Wu, and Dario Amodei. Scaling laws for neural language models, 2020.
- Tali Kaufman and Dana Ron. Testing polynomials over general fields. *SIAM J. Comput.*, 36: 779–802, 10 2006. doi: 10.1137/S0097539704445615.
- Lauro Langosco Di Langosco, Jack Koch, Lee D Sharkey, Jacob Pfau, and David Krueger. Goal misgeneralization in deep reinforcement learning. In Kamalika Chaudhuri, Stefanie Jegelka, Le Song, Csaba Szepesvari, Gang Niu, and Sivan Sabato, editors, *Proceedings of the 39th International Conference on Machine Learning*, volume 162 of *Proceedings of Machine Learning Research*, pages 12004–12019. PMLR, 17–23 Jul 2022. URL <https://proceedings.mlr.press/v162/langosco22a.html>.
- Jan Leike, David Krueger, Tom Everitt, Miljan Martic, Vishal Maini, and Shane Legg. Scalable agent alignment via reward modeling: a research direction, 2018.
- Andreu Mas-Colell, Michael D. Whinston, and Jerry R. Green. *Microeconomic Theory*. Oxford University Press, New York, 1995.
- Song Mei and Andrea Montanari. The generalization error of random features regression: Precise asymptotics and the double descent curve. 75(4):667–766. ISSN 1097-0312. doi: 10.1002/cpa.22008.
- Theodor Misiakiewicz and Andrea Montanari. Six Lectures on Linearized Neural Networks. *arXiv e-prints*, art. arXiv:2308.13431, August 2023. doi: 10.48550/arXiv.2308.13431.

- Richard Ngo, Lawrence Chan, and Sören Mindermann. The alignment problem from a deep learning perspective, 2024.
- Long Ouyang, Jeffrey Wu, Xu Jiang, Diogo Almeida, Carroll Wainwright, Pamela Mishkin, Chong Zhang, Sandhini Agarwal, Katarina Slama, Alex Ray, John Schulman, Jacob Hilton, Fraser Kelton, Luke Miller, Maddie Simens, Amanda Askell, Peter Welinder, Paul F Christiano, Jan Leike, and Ryan Lowe. Training language models to follow instructions with human feedback. In S. Koyejo, S. Mohamed, A. Agarwal, D. Belgrave, K. Cho, and A. Oh, editors, *Advances in Neural Information Processing Systems*, volume 35, pages 27730–27744. Curran Associates, Inc., 2022. URL https://proceedings.neurips.cc/paper_files/paper/2022/file/b1efde53be364a73914f58805a001731-Paper-Conference.pdf.
- Ethan Perez, Sam Ringer, Kamilė Lukošiuotė, Karina Nguyen, Edwin Chen, Scott Heiner, Craig Pettit, Catherine Olsson, Sandipan Kundu, Saurav Kadavath, Andy Jones, Anna Chen, Ben Mann, Brian Israel, Bryan Seethor, Cameron McKinnon, Christopher Olah, Da Yan, Daniela Amodei, Dario Amodei, Dawn Drain, Dustin Li, Eli Tran-Johnson, Guro Khundadze, Jackson Kernion, James Landis, Jamie Kerr, Jared Mueller, Jeeyoon Hyun, Joshua Landau, Kamal Ndousse, Landon Goldberg, Liane Lovitt, Martin Lucas, Michael Sellitto, Miranda Zhang, Neerav Kingsland, Nelson Elhage, Nicholas Joseph, Noemí Mercado, Nova DasSarma, Oliver Rausch, Robin Larson, Sam McCandlish, Scott Johnston, Shauna Kravec, Sheer El Showk, Tamera Lanham, Timothy Telleen-Lawton, Tom Brown, Tom Henighan, Tristan Hume, Yuntao Bai, Zac Hatfield-Dodds, Jack Clark, Samuel R. Bowman, Amanda Askell, Roger Grosse, Danny Hernandez, Deep Ganguli, Evan Hubinger, Nicholas Schiefer, and Jared Kaplan. Discovering language model behaviors with model-written evaluations, 2022.
- Dana Ron. Property testing: A learning theory perspective. *Found. Trends Mach. Learn.*, 1(3): 307–402, 2008. doi: 10.1561/2200000004. URL <https://doi.org/10.1561/2200000004>.
- Davor Runje and Sharath M. Shankaranarayana. Constrained monotonic neural networks, 2023.
- Rohin Shah, Vikrant Varma, Ramana Kumar, Mary Phuong, Victoria Krakovna, Jonathan Uesato, and Zac Kenton. Goal misgeneralization: Why correct specifications aren’t enough for correct goals, 2022.
- Toby Shevlane, Sebastian Farquhar, Ben Garfinkel, Mary Phuong, Jess Whittlestone, Jade Leung, Daniel Kokotajlo, Nahema Marchal, Markus Anderljung, Noam Kolt, Lewis Ho, Divya Siddarth, Shahar Avin, Will Hawkins, Been Kim, Iason Gabriel, Vijay Bolina, Jack Clark, Yoshua Bengio, Paul Christiano, and Allan Dafoe. Model evaluation for extreme risks, 2023.
- Joseph Sill and Yaser Abu-Mostafa. Monotonicity hints. In M.C. Mozer, M. Jordan, and T. Petsche, editors, *Advances in Neural Information Processing Systems*, volume 9. MIT Press, 1996. URL https://proceedings.neurips.cc/paper_files/paper/1996/file/c850371fda6892fbfd1c5a5b457e5777-Paper.pdf.

Pnar Tfekci and Heysem Kaya. Combined Cycle Power Plant. UCI Machine Learning Repository, 2014. DOI: <https://doi.org/10.24432/C5002N>.

Vladimir Vovk, Alexander Gammerman, and Glenn Shafer. *Algorithmic Learning in a Random World, Second Edition*. January 2005. doi: 10.1007/978-3-031-06649-8. Springer-Verlag New York, Inc. 2005.

Serena Wang and Maya Gupta. Deontological ethics by monotonicity shape constraints, 2020.

Jeff Wu, Long Ouyang, Daniel M. Ziegler, Nisan Stiennon, Ryan Lowe, Jan Leike, and Paul Christiano. Recursively summarizing books with human feedback, 2021.

Yasin Abbasi Yadkori, Ilja Kuzborskij, David Stutz, András György, Adam Fisch, Arnaud Doucet, Iuliya Beloshapka, Wei-Hung Weng, Yao-Yuan Yang, Csaba Szepesvári, Ali Taylan Cemgil, and Nenad Tomasev. Mitigating llm hallucinations via conformal abstention, 2024.

Seungil You, David Ding, Kevin Canini, Jan Pfeifer, and Maya Gupta. Deep lattice networks and partial monotonic functions, 2017.

A Proof of multi-lambda conformal risk control

Proof of Proposition 1. Our proof closely mimics the original proof of bounded risk found in [Angelopoulos et al. \[2024\]](#).

Proof. Let

$$\hat{R}_{n+1}(\boldsymbol{\lambda}) = \frac{(L_1(\boldsymbol{\lambda}) + \dots + L_{n+1}(\boldsymbol{\lambda}))}{(n+1)} \quad \text{and}$$

$$\begin{aligned} \mathbf{\Lambda}_{\min} &= \text{Min} \left\{ \boldsymbol{\lambda} \in \mathbf{\Lambda} : \hat{R}_{n+1}(\boldsymbol{\lambda}) \leq \alpha \right\} \\ \hat{\boldsymbol{\lambda}}' &\in \arg \min_{\boldsymbol{\lambda} \in \mathbf{\Lambda}_{\min}} g(\boldsymbol{\lambda}) \end{aligned}$$

The fact that $\inf_{\boldsymbol{\lambda}} L_i(\boldsymbol{\lambda}) = L_i(\boldsymbol{\lambda}^{\max}) \leq \alpha$ and the fact that g is strictly increasing implies $\hat{\boldsymbol{\lambda}}'$ is well-defined almost surely. Since $L_{n+1}(\boldsymbol{\lambda}) \leq B$, we have

$$\hat{R}_{n+1}(\boldsymbol{\lambda}) = \frac{n}{n+1} \hat{R}_n(\boldsymbol{\lambda}) + \frac{L_{n+1}(\boldsymbol{\lambda})}{n+1} \leq \frac{n}{n+1} \hat{R}_n(\boldsymbol{\lambda}) + \frac{B}{n+1}.$$

So if $\boldsymbol{\lambda}$ is such that

$$\frac{n}{n+1} \hat{R}_n(\boldsymbol{\lambda}) + \frac{B}{n+1} \leq \alpha,$$

Then we know $\hat{R}_{n+1}(\boldsymbol{\lambda}) \leq \alpha$. So when there exists $\boldsymbol{\lambda} \in \mathbf{\Lambda}$ such that the above inequality holds, this implies that either $\hat{\boldsymbol{\lambda}}' \leq \hat{\boldsymbol{\lambda}}$ or $\hat{\boldsymbol{\lambda}} \in \mathbf{\Lambda}_{\min}$, which in either case implies $g(\hat{\boldsymbol{\lambda}}') \leq g(\hat{\boldsymbol{\lambda}})$. And if $\frac{n}{n+1} \hat{R}_n(\boldsymbol{\lambda}) + \frac{B}{n+1} > \alpha$ for all $\boldsymbol{\lambda} \in \mathbf{\Lambda}$, then we must have $\hat{\boldsymbol{\lambda}} = \boldsymbol{\lambda}^{\max} \geq \hat{\boldsymbol{\lambda}}'$.

So we have $g(\hat{\boldsymbol{\lambda}}') \leq g(\hat{\boldsymbol{\lambda}})$ almost surely. And since $L_i(\boldsymbol{\lambda})$ is non-increasing with respect to $g(\boldsymbol{\lambda})$ we have

$$\mathbb{E} \left[L_{n+1}(\hat{\boldsymbol{\lambda}}) \right] \leq \mathbb{E} \left[L_{n+1}(\hat{\boldsymbol{\lambda}}') \right].$$

Let $E = \{L_1, \dots, L_{n+1}\}$, where $L_{n+1}(\boldsymbol{\lambda}) \mid E \sim \text{Uniform}(E)$ by exchangeability, and $\hat{\boldsymbol{\lambda}}'$ is constant conditional on E . Then with the right-continuity of L_i in each dimension we have

$$\mathbb{E} \left[L_{n+1}(\hat{\boldsymbol{\lambda}}') \mid E \right] = \frac{1}{n+1} \sum_{i=1}^{n+1} L_i(\hat{\boldsymbol{\lambda}}'_i) \leq \alpha.$$

Then applying the law of total expectation and our inequality from above we have

$$\mathbb{E} \left[L_{n+1}(\hat{\boldsymbol{\lambda}}) \right] \leq \alpha,$$

completing the proof. □

B Additional Examples

B.1 Additional monotonicity examples

We present more examples of the conformal alignment procedure for monotonicity from Section 4.1. We keep everything the same in terms of 70-15-15 train-calibrate-test split, averaging over 10 runs, and using XGBoost regression models. All experiments were run on an Apple M1 MacBook Pro. We train one constrained model on the train and calibration sets and one unconstrained model on the training set. We use default parameters without hyperparameter tuning. We use the same POT \mathbb{T} to obtain loss functions for applying conformal risk control on the unconstrained model using the calibration set.

Table 2: Abalone, $n = 4177$. Monotonically increasing on Shell_weight. $\boldsymbol{\lambda}^{\max} = (5, 5)$. $g(\boldsymbol{\lambda}) = \lambda^+ + \lambda^-$.

α	$\boldsymbol{\lambda}$	Metric	Unconstrained	Conformal	Constrained
0.1	$\lambda^+ = 0.07$	MSE	5.49	5.49	5.38
	$\lambda^- = 0.00$	Risk	0.096	0.093	0
0.05	$\lambda^+ = 0.29$	MSE	5.49	5.60	5.38
	$\lambda^- = 0.47$	Risk	0.096	0.062	0
0.01	$\lambda^+ = 0.63$	MSE	5.49	6.83	5.38
	$\lambda^- = 1.95$	Risk	0.096	0.018	0

B.2 Concavity results

We report the results of applying the conformal alignment procedure for the property of concavity using Algorithm 2 as our POT. Implementation details are the same as for the

Table 3: Concrete, $n = 1030$. Monotonically increasing on Cement. $\lambda^{\max} = (2, 2)$. $g(\lambda) = \lambda^+ + \lambda^-$.

α	λ	Metric	Unconstrained	Conformal	Constrained
0.1	$\lambda^+ = 0.004$	MSE	24.4	24.4	17.55
	$\lambda^- = 0.008$	Risk	0.081	0.081	0
0.05	$\lambda^+ = 0.092$	MSE	24.4	24.4	17.55
	$\lambda^- = 0.052$	Risk	0.081	0.075	0
0.01	$\lambda^+ = 0.710$	MSE	24.4	24.6	17.55
	$\lambda^- = 0.739$	Risk	0.081	0.043	0

monotonicity examples in Section 4.1 besides this change of POT and our procedure for choosing a specific point in order to measure performance on the accuracy metric, which here we take to be MAE. In this case our choice of the point prediction uses a scaling adjustment factor based on the position relative to the feature value at the maximum prediction, scaling from adding 0 to the predictions at the minimum feature value to adding λ to the prediction at the feature value of the maximum prediction, then adding 0 again at the maximum feature value. We re-emphasize, though, that the actual point prediction is not our main concern but rather the risk, which we can see matches the anticipated values well.

Table 4: Seoul Bike Sharing, $n = 8760$. Concave on temperature. $\lambda^{\max} = 100$.

α	λ	Metric	Unconstrained	Conformal
0.1	$\lambda = 28.8$	MAE	115	117
		Risk	0.31	0.090
0.05	$\lambda = 45.0$	MAE	114	119
		Risk	0.31	0.049
0.01	$\lambda = 84.2$	MAE	115	129
		Risk	0.31	0.011

C Details for a stylized examination of alignment persistence in AI models

We begin by describing the stylized model setting that can help us better understand the impact of overparameterization and data quality on a model’s ability to satisfy a property.

Notation. We consider feature vectors X to be samples from the uniform distribution on the sphere of radius \sqrt{d} in \mathbb{R}^d , that is denoted by $\mathbb{S}^{d-1}(\sqrt{d})$. For a function f , defined on a domain of the random variable X , we define its L^2 norm by $\|f\|_{L^2}^2 = \mathbb{E}_X[f(X)^2]$ where the expectation is with respect to the randomness in X . The notation $o_{n,\mathbb{P}}(1)$ for a positive integer means a quantity that goes to zero as n goes to infinity.

C.1 Noisy data setting

Data model. Consider a model where the data is generated according to the following equation,

$$y = g(X) + h(X) + \varepsilon,$$

where ε has mean 0 and variance τ^2 and is independent of X . Assume that $h(X)$ represents ‘bad’ data that is undesired and we do not want to learn. That is, we only want to learn $g(X)$, but there is a presence of biased noise, $h(X)$, in the data generating model.

Relating this to an alignment setting, domain experts expect the data to be generated according to $g(X) + \textit{unbiased noise}$, such that $g(X)$ exhibits some desired property \mathcal{P} . However, the data is generated according to $g(X) + \textit{biased noise}$, potentially obscuring the desired behavior. One potential reason for the presence of biased noise in data could be due to a measurement error of the outcome that is correlated with select features, leading to an incorrectly calculated outcome. A biased measurement error could occur if there is incomplete data and the presence of the incomplete data is correlated with select features in an unexpected, systematic way (e.g., it could hypothetically be correlated to the type of hospital or location at which a patient is treated).

The goal of these analyses is then to examine the impact of the noise bias term on a model’s ability to describe a behavior that is upheld by $g(X)$, but not necessarily $g(X) + h(X)$, across model complexity. For example, $g(X)$ might be monotonically increasing in the first coordinate of \mathbf{x} , but the summation of $g(X) + h(X)$ is not always. We will then try to draw conclusions about the distance between two kinds of models: one that is trained regularly without additional constraints, and another where we add a constraint to the training that forces the model to replicate the behavior of $g(X)$, despite $h(X)$. In the stylized model, when referring to the ‘distance’ between two models, we consider it to be zero if their learned parameters are the same, and non-zero if their learned parameters are different, when trained on the same data.

Learning method. We will assume we have access to a data set of n iid samples $\{(X_i, Y_i)\}_{i=1}^n$ obtained from the above data generating model, i.e., $Y_i = g(X_i) + h(X_i) + \varepsilon_i$. We denote this data set by D_n .

The function class we use to fit the data is the random feature model, which can be thought of as a two-layer neural network, with N hidden nodes, with the weights of the first layer set randomly, while the second layer weights are learned. This means the function class can be written as:

$$f_{\text{RF}}(X; \mathbf{a}, \{\mathbf{w}_j\}_{j \in [N]}) = \frac{1}{\sqrt{N}} \sum_{j \in [N]} a_j \sigma(\langle X, \mathbf{w}_j \rangle), \quad (2)$$

where $\mathbf{a} \in \mathbb{R}^N$ denotes the second layer weights and $\sigma(\cdot) : \mathbb{R} \rightarrow \mathbb{R}$ is a non-linear activation function. The random weights $\{\mathbf{w}_j\}_{j \in [N]}$ are such that each \mathbf{w}_j is an iid sample from a fixed distribution. For brevity, we drop the reference to \mathbf{a} and \mathbf{w}_j 's and use $f_{\text{RF}}(X)$ or $f_{\text{RF}}(X; \mathbf{a})$.

For the stylized model analysis, we consider a random feature model, because this function class has been studied in recent theory of deep learning models, and has shown some of the specific properties of modern overparameterized deep learning models such as concepts of benign overfitting and double descent [Mei and Montanari, Misiakiewicz and Montanari \[2023\]](#). We can thereby use this recent literature as a theoretical foundation to explain the potential impact of model complexity on model's ability to satisfy a property in large train set sizes.

Interestingly, the squared loss function for this problem is convex and we can minimize it by ridge regression. Mathematically, this means for any regularization parameter, λ , we will search for a vector of real numbers $\hat{\mathbf{a}}_\lambda \in \mathbb{R}^N$ such that,

$$\hat{\mathbf{a}}_\lambda = \arg \min_{\mathbf{a} \in \mathbb{R}^N} \sum_{i \in [n]} (Y_i - f_{\text{RF}}(X_i))^2 + \lambda \|\mathbf{a}\|_2^2. \quad (3)$$

C.2 RF theory

Assume a certain property, denoted by \mathcal{P} such that the function $g(X)$ satisfies \mathcal{P} . However, assume that $h(X)$ is such that $g(X) + h(X)$ does not satisfy \mathcal{P} .

Assume there is a way of constraining the training of $f_{\text{RF}}(X)$ to satisfy the \mathcal{P} . More formally, assume $C_{\mathcal{P}} \subset \mathbb{R}^N$ is the set of all coefficients \mathbf{a} such that $f_{\text{RF}}(X; \mathbf{a})$ satisfies \mathcal{P} , i.e.,

$$C_{\mathcal{P}} = \{\mathbf{a} \mid \mathbf{a} \in \mathbb{R}^N \text{ and } f_{\text{RF}}(X; \mathbf{a}) \text{ satisfies } \mathcal{P}\}.$$

Then we can consider the following constrained version of the model:

$$\hat{\mathbf{a}}_{\lambda, \mathcal{P}} = \arg \min_{\mathbf{a} \in C_{\mathcal{P}}} \sum_{i \in [n]} (Y_i - f_{\text{RF}}(X_i))^2 + \lambda \|\mathbf{a}\|_2^2. \quad (4)$$

Now assume that the functions g and h are polynomials such that $\deg_g < \deg_h$. Further assume that $n > d^{\deg_h + \delta}$, where δ is some small positive constant (e.g., $\delta = 0.1$) and that d is sufficiently large. Also assume that the activation function σ upholds the following genericity conditions (as stated and assumed in Theorem 3 in Section 4.2 of [Misiakiewicz and Montanari \[2023\]](#)): 1) $|\sigma(x)| \leq c_0 \exp(c_1|x|)$ for constants $c_0, c_1 > 0$; 2) for any $k \geq 0$, σ has a non-zero Hermite coefficient $\mu_k(\sigma) := \mathbb{E}_G\{\sigma(G)\text{He}_k(G)\} \neq 0$ (where $G \sim \mathcal{N}(0, 1)$ and He_k is the k -th Hermite polynomial, with the standard normalization $\langle \text{He}_j, \text{He}_k \rangle_{L^2(\mathcal{N}(0,1))} = k! \mathbb{1}_{\{j=k\}}$).

To analyze the impact of model complexity on a model's adherence to \mathcal{P} , we consider two settings for the stylized model:

- **Classic:** $d^{\deg_g + \delta} < N < d^{\deg_h - \delta}$.
- **Underspecified:** $N > d^{\deg_h + \delta}$.

To formalize our results, we will in part rely on Theorem 3 in Section 4.2 of [Misiakiewicz and Montanari \[2023\]](#). This theorem illustrates the roles that the number of hidden nodes, N , and the number of data points, n , play in determining the test error that can be achieved by a random feature model when approximating a function. Given the assumptions made in their work, in the setting where $N \ll n$, the number of hidden nodes, N , will limit the test error, while if $n \ll N$, the number of data points, n , will limit the test error [Misiakiewicz and Montanari \[2023\]](#). Building on this intuition, we first state an informal implication of this theorem [Misiakiewicz and Montanari \[2023\]](#) applied to our stylized model: under the same assumptions made in their work, for a sufficiently large d , in the classic setting, there exists a range of regularization parameters $[0, \lambda^*]$ such that for all λ in that range, $f_{\text{RF}}(X; \hat{\mathbf{a}}_\lambda)$ will learn a polynomial of at least \deg_g , but strictly less than \deg_h . But in the underspecified setting, $f_{\text{RF}}(X; \hat{\mathbf{a}}_\lambda)$ learns both parts $g(X)$ and $h(X)$, for all λ in a different range of regularization parameters $[0, \lambda^*]$, meaning it learns the noise bias. This means, in a large data domain, the behavior of the classic and underspecified setting is different.

In order to formalize this intuition for the underspecified setting, we need to state an assumption on the degree of violation of property \mathcal{B} around the function $g + h$.

Assumption 1 (Property Unsatisfied in a Neighborhood). *There exists a positive constant R such that, for all \mathbf{a}' with $\|(g + h) - f_{\text{RF}}(\cdot; \mathbf{a}')\|_{L^2} \leq R$, the function $f_{\text{RF}}(X, \mathbf{a}')$ does not satisfy the property \mathcal{P} .*

Theorem 2 (Non-vanishing Distance in Underspecified Setting). *Assume $N > d^{\deg_h + \delta}$, $n > d^{\deg_h + \delta}$, $\max(N/n, n/N) \geq d^\delta$ for a constant $\delta > 0$, Assumption 1 holds, σ upholds the genericity conditions stated above, and d is sufficiently large. Then, in the underspecified setting, there exists a constant λ^* , such that for any $\lambda \in [0, \lambda^*]$ the following holds:*

$$\hat{\mathbf{a}}_{\lambda, \mathcal{P}} \neq \hat{\mathbf{a}}_\lambda. \quad (5)$$

Proof. Using Theorem 3 of [Misiakiewicz and Montanari \[2023\]](#), we have that

$$\|(g + h) - f_{\text{RF}}(\cdot; \hat{\mathbf{a}}_\lambda)\|_{L^2}^2 = o_{d, \mathbb{P}}(1) \cdot (\|g + h\|_{L^{2+\eta}}^2 + \tau^2).$$

for all $\eta > 0$. With d sufficiently large, the square root of the quantity on the right hand side will be less than R , which combined with Assumption 1, means $f_{\text{RF}}(\cdot; \hat{\mathbf{a}}_\lambda)$ does not satisfy \mathcal{P} , and therefore, $\hat{\mathbf{a}}_\lambda \notin C_{\mathcal{P}}$. \square

Under two additional assumptions, we can further state a result showing that in the classic setting, for a given range of regularization parameters, we will be able to learn the property \mathcal{P} . At a high level, these assumptions are that 1) the overall impact of h is small, for example, when it only impacts a small portion of the data; and 2) the property \mathcal{P} is preserved in a small neighborhood of g among the function class learned in the classic setting. Formalizing the assumptions and stating the result:

Assumption 2 (Small Noise Bias). Assume there is a small constant ϵ_h such that

$$\|h\|_{L^2} \leq \epsilon_h.$$

Assumption 3 (Property Robustness in Function Class). For any fixed N , there exists a positive constant R_N such that, for all \mathbf{a}' with $\|g - f_{\text{RF}}(\cdot; \mathbf{a}')\|_{L^2} \leq R_N$, the function $f_{\text{RF}}(X, \mathbf{a}')$ satisfies the property \mathcal{P} .

Theorem 3 (Zero Distance in Classic Setting). Assume $d^{\text{deg}_g + \delta} < N < d^{\text{deg}_h - \delta}$, $n > d^{\text{deg}_h + \delta}$, $n/N \geq d^\delta$ for a constant $\delta > 0$, Assumptions 2-3 hold, σ upholds the genericity conditions, d is sufficiently large, and $R_N > 2\epsilon_h$. Then, in the classic setting, there exists a constant λ^* , such that for any $\lambda \in [0, \lambda^*]$, the following holds:

$$\hat{\mathbf{a}}_{\lambda, \mathcal{P}} = \hat{\mathbf{a}}_\lambda. \quad (6)$$

Proof. Using the triangle inequality and Theorem 3 of [Misiakiewicz and Montanari \[2023\]](#) again, we have that

$$\begin{aligned} \|f_{\text{RF}}(\cdot; \hat{\mathbf{a}}_\lambda) - g\|_{L^2}^2 &\leq 2(\|f_{\text{RF}}(\cdot; \hat{\mathbf{a}}_\lambda) - g - h\|_{L^2}^2 + \|h\|_{L^2}^2) \\ &\leq 4\|h\|_{L^2}^2 \\ &\leq 4\epsilon_h^2. \end{aligned}$$

Taking the square root, the right hand side of the last term is less than R_N which combined with Assumption 3 means $f_{\text{RF}}(\cdot; \hat{\mathbf{a}}_\lambda)$ satisfies property \mathcal{P} . \square

Remark 1. Note that the constant R_N will converge to zero as N grows, meaning the assumption $R_N > 2\epsilon_h$ will break down when N is large. For example, in the underspecified setting, this assumption breaks down and hence the distance does not vanish.

C.3 Synthetic validation under a relaxed assumption on the noise bias, and conformal correction

In this section, we first numerically validate the above theoretical results, in a setting that noise bias only impacts a small fraction of the pre-training data. Next, we apply our proposed procedure of alignment through conformal risk control. We take the desired property \mathcal{P} to be monotonicity and use the same procedure as on the real-world datasets in Section 4.1.

We consider $g(X) = \langle X, \beta \rangle$ with β a constant in \mathbb{R}^d with $\beta_1 > 0$ and $\|\beta\|_2 = 1$. Then let $h(X) = \min(M, \alpha Z_p x_1^4)$ where Z_p is a Bernoulli random variable with a success probability p , that is sampled independently for each data point, and α and M are positive constants. This function is aimed to model a biased noise that is capped by magnitude M and only applies to a fraction p of the population. This is to mimic characteristics of a real dataset where only a portion of the data might have the bias (i.e., ‘bad’ data). This is therefore capturing a more realistic case of the stylized model setting, where the measurement error may only occur for a small subset of the data.

Using a large train set size, we fit the data generated according to the outcome model above using the random feature model with λ tuned via cross-validation, assuming the

ReLU activation function, i.e., $\sigma(x) = \max(0, x)$, and \mathbf{w}_j is iid $\mathcal{N}(0, 1)$. We then assess how model complexity affects whether the predicted function is monotone in x_1 by looking at the univariate partial dependence plot of the predicted function versus the (counterfactual) unbiased outcome, $g(X)$, for the first coordinate x_1 . We vary model complexity by N , the number of hidden nodes in the model.

Applying this synthetic simulation for specific parameters, Figure 2 shows that when training a relatively simple model ($N = 5$) on the generated data, the model describes a monotonically increasing relationship. From this we conclude that if we had constrained the model to uphold monotonicity in x_1 , it would not have changed the final model’s parameters. Hence, the distance between the constrained and unconstrained model would be zero and we require no conformal correction. In contrast, as seen in Figure 3, a more complex model ($N = 5000$) predicts a non-monotone relationship, and therefore, if we had constrained the model to uphold monotonicity in x_1 , it would have changed the final model’s parameters, such that the distance between the constrained and unconstrained model would be non-zero and we do require a conformal correction to post-process and align this model.

The synthetic simulation seems to validate that with a seemingly large training dataset, increasing model complexity, on the one hand, can enable high performance, but can also make ML models more sensitive to small noise bias in the data, which can subsequently lead to model behavior inconsistent with requirements by the end-user.

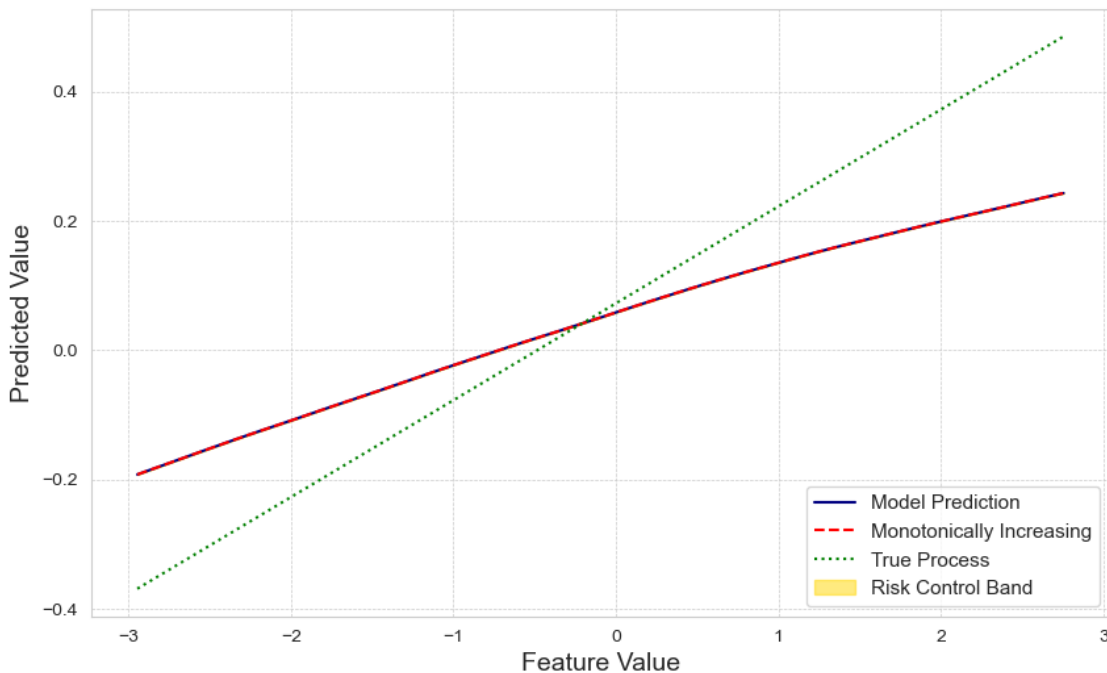


Figure 2: Random Feature model ($N=5$).

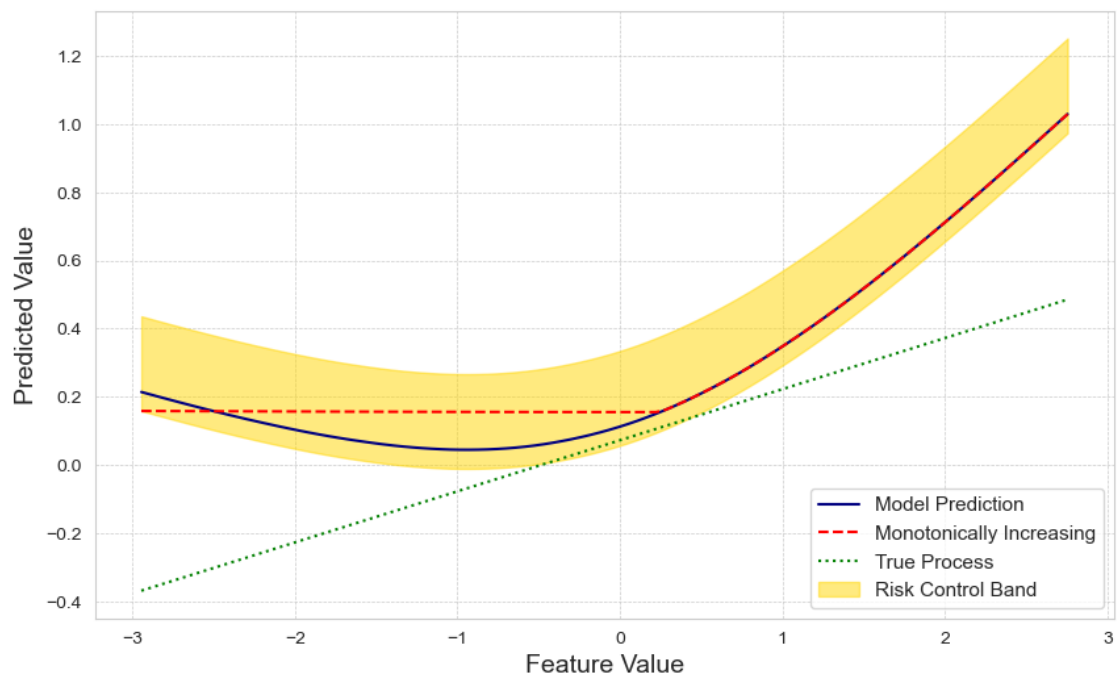


Figure 3: Random Feature model (N=5000).